Supporting Information

Amplification-free, OR-gated CRISPR Cascade reaction for pathogen detection in blood samples

Jongwon Lim[a,b], An Bao Van[a,b,c], Katherine Koprowski[a,b], Matthew Wester[a,b], Enrique Valera[a,b,d], Rashid Bashir[a,b,d,e,f,g,h,i,*]

[a] Department of Bioengineering, University of Illinois at Urbana–Champaign, Urbana, IL 61801, United States

[b] Nick Holonyak Jr. Micro and Nanotechnology Laboratory, University of Illinois at Urbana–Champaign, Urbana, IL 61801, United States

[c] VinUni-Illinois Smart Health Center, Building G, VinUni Campus, Vinhomes Ocean Park, Gia Lam Dist, Hanoi, Vietnam

[d] Carl R. Woese Institute for Genomic Biology, University of Illinois at Urbana–Champaign, Urbana, IL 61801, United States

[e] Department of Mechanical Science and Engineering, University of Illinois at Urbana–Champaign, Urbana, IL 61801, United States

[f] Department of Electrical and Computer Engineering, University of Illinois at Urbana–Champaign, Urbana, IL 61801, United States

[g] Department of Materials Science and Engineering, University of Illinois at Urbana–Champaign, Urbana, IL 61801, United States

[h] Department of Biomedical and Translational Sciences, Carle Illinois College of Medicine, Urbana, IL 61801, United States

[i] Chan Zuckerberg Biohub Chicago, Chicago, IL 60642

*Corresponding Authors: R.B. (rbashir@illinois.edu).

Table S1. Nucleic acid sequences for Cascade reaction

Oligo ID	Sequences
Blocked nucleic acid	GGATATACTTTTTATTTTTGATAAATATATATATTTTTATTTTTATATATATATATCGTATATCC
gRNA for RNP T2	UAAUUUCUACUAAGUGUAGAUGGAUAUACGAUAUAUAUAUAU
gRNA for RNP T1 >> MRSA	UAAUUUCUACUAAGUGUAGAUGGUCUAAAAUUUUACCACGU
gRNA for RNP T1 >> MSSA	UAAUUUCUACUAAGUGUAGAUUUACACAUAUGUUCUUCCCUAAUAACAG
gRNA for RNP T1 >> E coli	GGGUAAUUUCUACUAAGUGUAGAUCCAACCGUCAUUGACAGGAA
gRNA for RNP T1 >> HBV	UAAUUUCUACUAAGUGUAGAUCGGAAGUGUUGAU AGGAUAG
MRSA mecA gene Fragment sequences	ACGTGGTAAAATTTTAGACCATCTACACTTAGTAGAAATTACCCTATAGTGAGTCGTATTA
Reporter	/56-FAM/TT TTT T/3IABkFQ/

Table S2. BNA modifications

Oligo ID	Sequences
Modi 1	GGA TAT ACT TTT TAT TTT TGA TAA ATA TAT ATA TTT TTA TTT TTA TAT ATA TAT ATC GTA T/iBiodT/A TCC
Modi 2	GGA TAT ACT TTT TAT TTT TGA TAA ATA TAT ATA TTT TTA TTT TTA TAT ATA TAT ATC GTA TAT /iBiodT/CC
Modi 3	GGA TAT ACT TTT TAT TTT TGA TAA ATA TAT ATA TTT TTA TTT TTA TAT ATA TAT ATC GTA TAT CC/3BiodT/
Modi 4	AGG ATA TAC TTT TTA TTT TTG ATA AAT ATA TAT ATT TTT ATT TTT ATA TAT ATA TAT CGT ATA TCC T/3BiodT/
Modi 5	TAG GAT ATA CTT TTT ATT TTT GAT AAA TAT ATA TAT TTT TAT TTT TAT ATA TAT ATA TCG TAT ATC CTA /3BiodT/
Modi 6	GTA GGA TAT ACT TTT TAT TTT TGA TAA ATA TAT ATA TTT TTA TTT TTA TAT ATA TAT ATC GTA TAT CCT AC/3BiodT/

Table S3. Summary of the CRISPR-Cascade diagnostic papers.

Ref	26	27	45	46	This paper
Sensitivity or LOD	5 atto molar	1 atto molar	1 atto molar	50 femto molar	1 atto molar
SNR	3	5 - infinite	1.2	4	1.3
Detection time	4 hours	20 min	15 min - 1 hour	1 hour	10 min
Temperature	37	33	RT	37	33
Quantification	atto - nano	atto molar range	See below (1)	femto -pico	1 - 100 atto molar
BNA Design	3 components	2 components	circular	split activator	1 component
BNA concentration	High (1uM)	Low (100nM)	Low (50nM)	Low (50nM)	Low (100nM)
Nonspecific signal	Yes	Yes	Yes	Yes	Yes
Specialty	First paper	Multiple region target	No	LNA and specific cleavage	See below (2)
Or gate functionality	No	Within SARS-CoV-2	No	No	4 pathogens
Sample type	HBV infected cells (not blood)	Swab	Plasma	Cell	Blood

1) 1 -100 atto-molar/ 0 - 1 copy/μL of H. pylori genome DNA/ 1 - 10 copies/μL of SARS-CoV-2 genomic RNA

2) Steric hindrance (human genomic DNA & biotin modification)

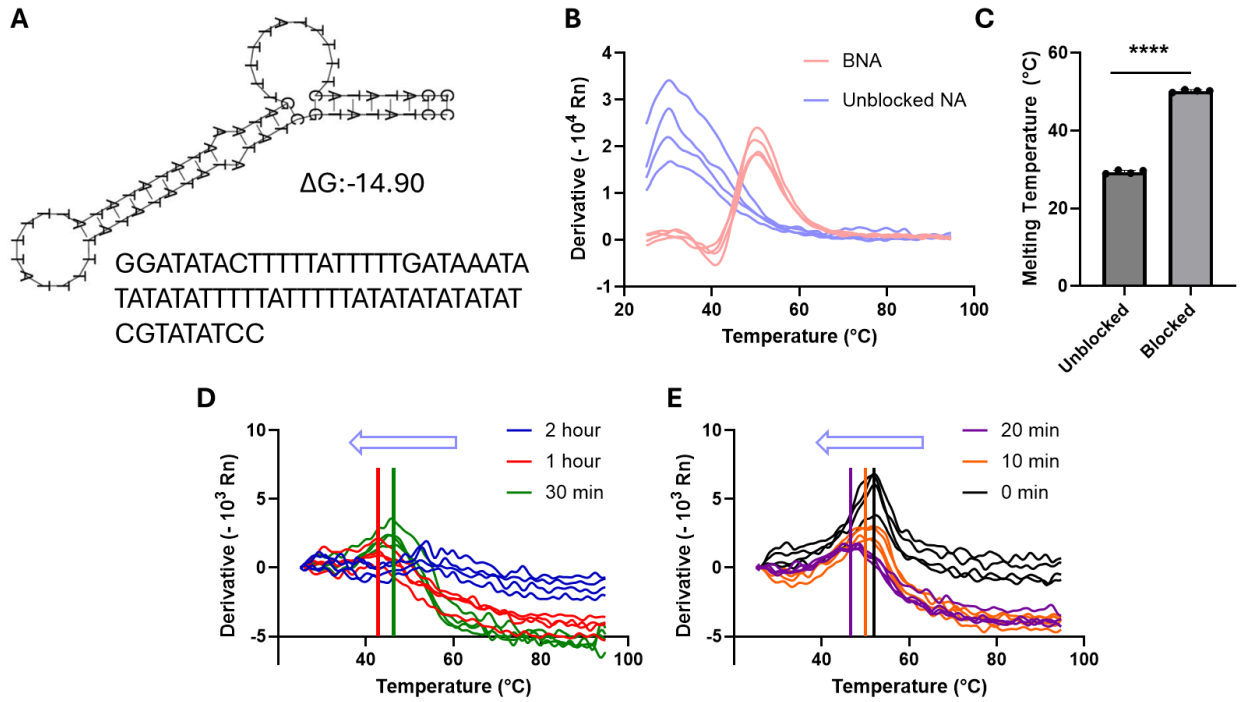


Figure S1. Characterization of BNA and RNP T2's mechanism of a positive feedback loop activation. (A-C) Secondary structure formed by single stranded DNA sequences of BNA when incubated with buffers promoting base pairings. (A) BNA structure with 4 hours incubation. (B) Melting curve analysis. (C) Enhanced thermal stability of blocked nucleic acids observed after a 4-hour room temperature pre-incubation in a buffered solution promoting secondary structures. (D-E) Melting curve analysis of BNA after incubation with activated RNP T2 complex for 2 hours, 1 hour, 30 minutes, and 10 minutes shows a gradual peak shift as reaction time increases. This indicates the cleavage of single-stranded BNA bulges, which destabilizes the BNA molecules and leads to the denaturation of the targeted nucleic acid sequences. (E) Consequently, the shielding effect decreases, resulting in reduced melting temperatures. Data is presented individually for each instance. Statistical significance is indicated as follows: *p < 0.05, **p < 0.01, ***p < 0.001, ****p < 0.0001, based on a two-tailed P value from an unpaired t-test.

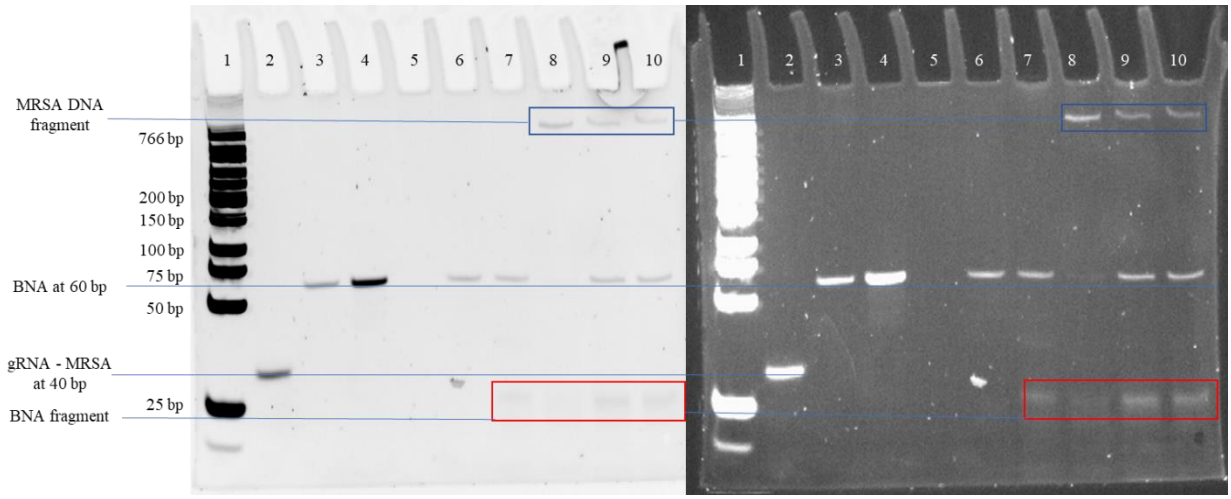


Figure S2. Characterization of gel electrophoresis analysis of the CRISPR Cascade reaction components and products. A low-molecular weight ladder (NEB, N3233S) was utilized for size reference. The two gel images represent the same gel but were captured using different image settings. The gel lanes were loaded as follows: 1) NEB low-molecular weight ladder, 2) RNP T1's MRSA gRNA (100 nM), 3) Unblocked, fresh, nucleic acid (NA) sequence (100 nM), 4) NA incubated for 4 hours at RT in salt solution (100 nM)—forming secondary DNA structure called BNA, 5) MRSA DNA (10^4 copies/µL), 6) RNPT1 (LbCas12a complexed to gRNA for MRSA) with MRSA DNA (10^4 copies/µL) and BNA (100 nM), 7) RNPT2 (LbCas12a complexed to gRNA for RNP T2) with BNA (100 nM), 8) Full Cascade reaction (with 10^4 copies/µL MRSA and 100 nM BNA), 9) and 10) Full cascade reaction (with 10^4 copies/µL MRSA and 1 µM BNA). The samples loaded in lanes 6-10 were taken from single CRISPR or Cascade reactions incubated for 30 minutes at 33C without reporter present.

Supplementary Note: Gel electrophoresis analysis for CRISPR Cascade reaction

The length of our MRSA gRNA MRSA is 41 base pairs, consistent with its migration to between the 25 and 50 bp lanes in the ladder. Our SYBR 1 gel stain can intercalate between ds regions of the gRNA, specifically the small direct repeat loop in the handle segment.[1]

BNA Migration: The length of BNA sequence is 65 bps. Both the fresh unincubated NA sequence and the BNA consistently migrated to a position corresponding to 60 bp relative to the ladder.

The Lane 3 fresh NA should be mostly ssDNA, while the Lane 4 blocked nucleic acid should mostly be the dsDNA folded version of the ssDNA. Both lanes 3 & 4 migrate about the same because the pore diameter of the 15% gel with 3%C (120 nM)[2] is too large to distinguish between the unfolded and folded states of the DNA (diameter=1-2 nM).[3] Another possibility is that either, during the process of diluting the samples of lane 3&4 in loading dye, or during the gel run itself, the change in ionic conditions and the need to navigate the gel as efficiently as possible caused a change in the conformation of either sample so that they would migrate about the same distance. However, we do see a change in intensity of lane 4 compared to lane 3. Since SYBR Green 1 specifically intercalates between dsDNA, this could imply that after the 4 hr incubation, there is a higher concentration of dsDNA present.

MRSA DNA: In lane 5, no band is visible, suggesting that the MRSA DNA (genomic DNA from MRSA strain HFH-30106, NR-10320), which has a length of approximately 2.8 Mbp, had a molecular weight too large to be resolved by the PAGE.

CRISPR Reaction Products:

- Lane 6 (RNPT1 with 10^4 copies/µL MRSA and 100 nM BNA): We do not see the MRSA gRNA in this lane because all or most of it is complexed to the Cas12 enzyme, which is too large to get through the gel and will not be stained by SYBR 1. BNA is still present in this lane, while there are no bands of cut BNA fragments as shown in lanes 7-10 because RNPT2 is not present in the reaction. There is also not a MRSA cut fragment in this lane as there is in lanes 7-10 since 10^4 copies/µL is around the limit of detection (LOD) of single CRISPR, and the concentration of cut MRSA may be too low to see in PAGE.
- Lane 7 (RNPT2 with BNA): Again, no band for gRNA for RNP T2 because it is mostly complexed to the Cas12 enzyme which won't be visible in this type of PAGE. A minor fraction of BNA cleavage was observed, with the appearance of fragments around 25 bp, demonstrating the successful RNPT2 cleavage of BNA at the ssDNA loops.
- Lane 8 (full Cascade reaction, 10^4 copies/µL MRSA, 100 nM BNA): Complete consumption of BNA was evident, accompanied by the presence of fragments at approximately 25 bp. Bands/smear at 30 bps reveal trans cleavage of BNA by both activated RNPT1 and RNPT2. Band at 766 bp is the cleaved MRSA dsDNA fragment cut via cis cleavage by RNPT1.
- Lanes 9-10 (Complete Cascade reaction, 10^4 copies/µL MRSA, 1 µM BNA): Lanes 9/10 are replicates of the entire CRISPR Cascade system, this time instead including 1 µM of BNA (a higher concentration than what we usually use for the R mix) to better visualize the BNA cleavage products. Again, we see the large MRSA cut gene fragment at the top, the BNA band at 60 bps, and the BNA cleavage products with the band size of about 30 bps.

The gel electrophoresis results provide evidence for the functionality of the CRISPR Cascade reaction. The observed BNA cleavage and the generation of specific fragment sizes indicate the successful implementation of a positive feedback loop mechanism. This amplification system effectively consumes BNA during the reaction, potentially enhancing the sensitivity and signal output of the CRISPR-based detection method for MRSA DNA.

PAGE Protocol:

The 15% nondenaturing polyacrylamide gel was hand cast using the Biorad Mini-Protean Tetracell system following their 15% gel recipe/protocol using TEMED (1610800), 10% wt/vol APS (1610700), and 40% Acrylamide and bis-acrylamide gel solution, 29:1 (1610146). After casting, we loaded the samples using the NEB Gel loading dye, purple 6X, no SDS (B7025) and ran the gel in 1XTBE (ThermoFisher, 161-0733) at 100V for 2 hours. We then stained the gel with 10,000x diluted ThermoFisher SYBR 1 gel stain (S7563) in 1XTBE for 40 minutes on a shaker, and imaged it using Biorad Gel Doc XR+ Imaging System.

References:

1. Bandyopadhyay, A., Kancharla, N., Javalkote, V. S., Dasgupta, S., & Brutnell, T. P. (2020). CRISPR-Cas12a (Cpf1): a versatile tool in the plant genome editing tool box for agricultural advancement. *Frontiers in plant science*, *11*, 584151.
2. Holmes, D. L., & Stellwagen, N. C. (1991). Estimation of polyacrylamide gel pore size from Ferguson plots of linear DNA fragments. II. Comparison of gels with different crosslinker concentrations, added agarose and added linear polyacrylamide. *Electrophoresis*, *12*(9), 612-619.

3. Ambia-Garrido, J., Vainrub, A., & Pettitt, B. M. (2010). A model for structure and thermodynamics of ssDNA and dsDNA near a surface: A coarse grained approach. *Computer physics communications*, *181*(12), 2001-2007.

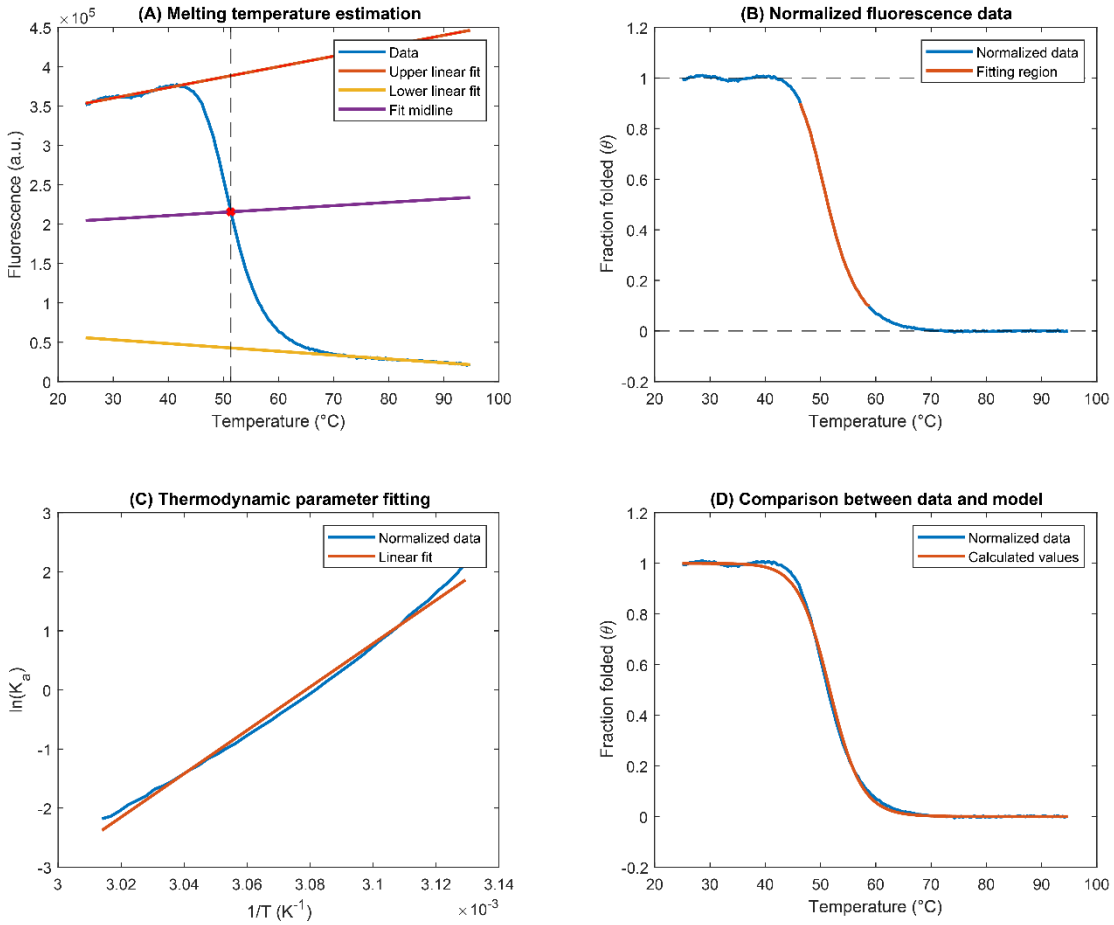


Figure S3. Melting curve thermodynamic analysis. (A) Estimation of the melting point based on the intersection of the melting curve with the linear fit midline. (B) Normalization of the melting point data before fitting. (C) Fitting of the thermodynamic parameters $\Delta H°$ and $\Delta S°$. (D) Comparison of the normalized data with the fraction calculated by the simplified thermodynamic data.

Supplementary Note: Melting curve thermodynamic analysis for blocked nucleic acid unfolding

While the melting temperature can generally indicate the tendency for an oligonucleotide to remain in the annealed state, it is not sufficient to predict the annealed or melted fraction across a range of temperatures. To supplement the melting temperature calculation, the melting curves for the blocked nucleic acid (BNA) were analyzed following the steps outlined by Mergny and Lacroix.[1] The process (using custom Matlab code) is visualized in Figure S2.

First, the linear regions at the upper and lower range of the melting curve are manually selected. A linear fit is applied to each using the polyfit function in Matlab (**Fig. S2A**). The midline between these linear fits is determined by averaging the slopes and y-intercepts. The intersection of the midline with the melting curve can be used to determine the melting temperature (here, 51.34 °C) as an alternative to the method based on the derivative of the melting curve. A normalization is applied according to:

$$y'(t) = \frac{y(t) - y_l(t)}{y_u(t) - y_l(t)}$$

with:

$$y_u(t) = m_u t + b_u$$
$$y_l(t) = m_l t + b_l$$

where $y'(t)$ is the transformed value, $y(t)$ is the initial value, and $y_u(t)$ and $y_l(t)$ are the upper and lower linear fits. This transforms the upper linear fit, midline, and lower linear fit to a fraction folded (θ) of 1, 0.5, and 0, respectively (**Fig. S2B**). The data for $0.1 < \theta < 0.9$ is isolated for further fitting.

The normalized data is then transformed from the form θ vs. T $(°C)$ to $\ln(K_a)$ vs. $1/T$ (K^{-1}) (**Fig. S2C**). K_a is the affinity constant for a two-state equilibrium, defined as:

$$K_a = \frac{\theta}{1-\theta}$$

Another linear fit is applied to this data using polyfit. The slope and y-intercept of the transformed data should be $-\Delta H°/R$ and $\Delta S°/R$, respectively, where $\Delta H°$ is the standard enthalpy change, $\Delta S°$ is the standard entropy change, and R is the gas constant. These allow us to calculate the Gibbs free energy change for a given temperature:

$$\Delta G(T) = \Delta H° - T\Delta S°$$

and consequently the fraction of BNA that is unfolded, or melted:

$$f_{unfolded}(T) = (1 - \theta(T)) = \frac{1}{1 + \exp(-\Delta G(T)/(RT))}$$

The calculated value for $f_{unfolded}$ is plotted against the normalized data in **Figure S2D** to demonstrate the general agreement.

This analysis relies on two key simplifications. First, it is assumed that the melting curve is measuring a two-state equilibrium between the melted and annealed blocked nucleic acid. This is generally an acceptable simplification for short hairpin oligonucleotides but may be less valid for a number of other cases covered by Mergny and Lacroix. Second, the enthalpy and entropy change values are assumed to be temperature independent. Consequently, there should also be no change in heat capacity during the reaction.

Across eight melting curve experiments, the calculated values were:

$\Delta H°$ (kcal/mol)	$\Delta S°$ (kcal/(mol K))
-72.96	-0.2246
-82.02	-0.2520
-77.04	-0.2359
-76.02	-0.2333
-79.08	-0.2429
-84.99	-0.2609

-83.03	-0.2547
-72.35	-0.2230

With average values of $\Delta H° = 78.44 \pm 4.36$ kcal/mol and $\Delta S° = -0.2409 \pm 0.0132$ kcal/(mol K).

At the reaction temperature of 33 °C, this results in $\Delta G = -4.683$ kcal/mol and an unfolded fraction $f_{unfolded} = 0.0004532$ or 0.045%. This means that for a starting oligonucleotide concentration of 100 nM, the initial unfolded concentration is approximately 45 pM. This initial unfolded concentration is likely to contribute to the significant background amplification in the reaction.

[1] J.-L. Mergny, L. Lacroix, Analysis of thermal melting curves. *Oligonucleotides* **13**, 515–537 (2003).

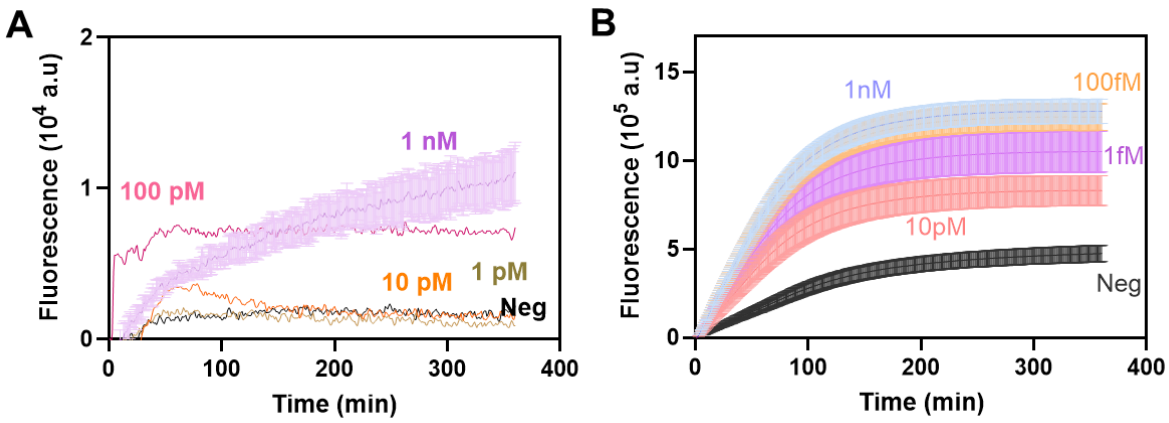


Figure S4. Fluorescence results from experiments where both reactions were incubated with a target fragment of the MRSA mecA gene for 360 minutes. (A) The single Cas12a reaction generates minimal fluorescence signal at a 1nM target concentration and fails to produce a signal below this range. (B) The Cascade reaction produces a strong fluorescence signal across a wider range of concentrations. Data are shown as individual points with mean ± SD (n=3), with bars indicating the mean value.

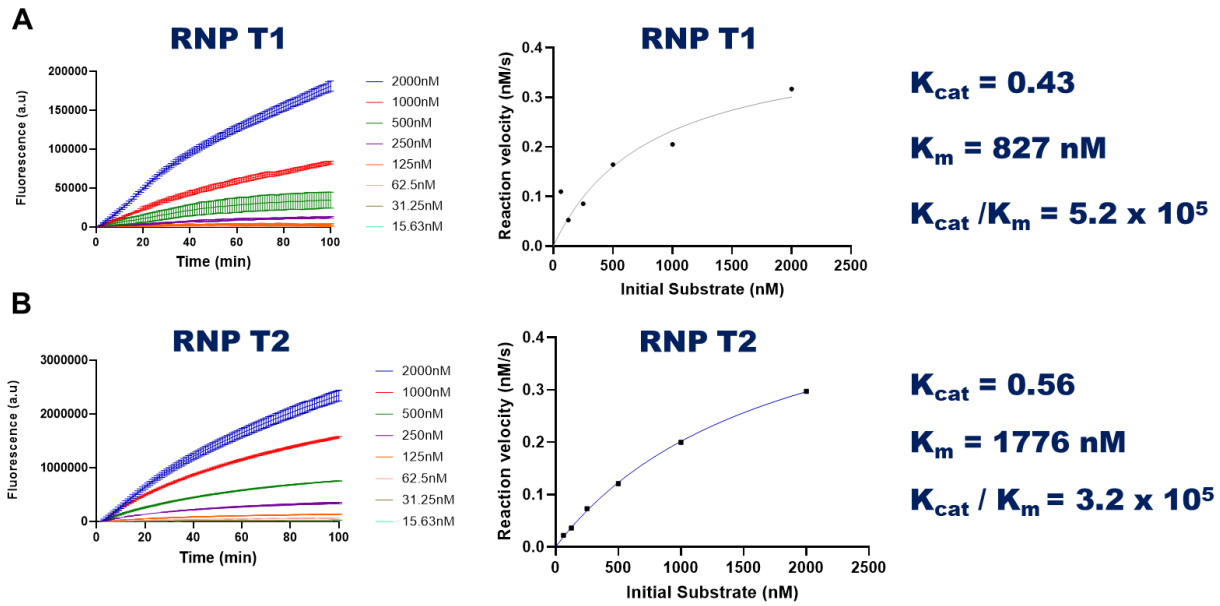


Figure S5. Enzyme and gRNA kinetic experiments were conducted to calculate the K_{cat} and K_m values for (A) RNP T1 and (B) RNP T2. Data are shown as mean ± SD (n=3), with bars representing the mean values. The reactions were tracked with measurements recorded every minute. A fluorescence calibration curve was employed to convert fluorescence readings into molar concentrations. Initial reaction velocities (nM per second) for Michaelis−Menten analysis were determined by applying a linear fit to the first 5 minutes of the reaction progress curves. The relationship between reaction velocities and reporter concentrations was fitted to the Michaelis−Menten equation using GraphPad Prism 10 to calculate the K_{cat} and K_m values.

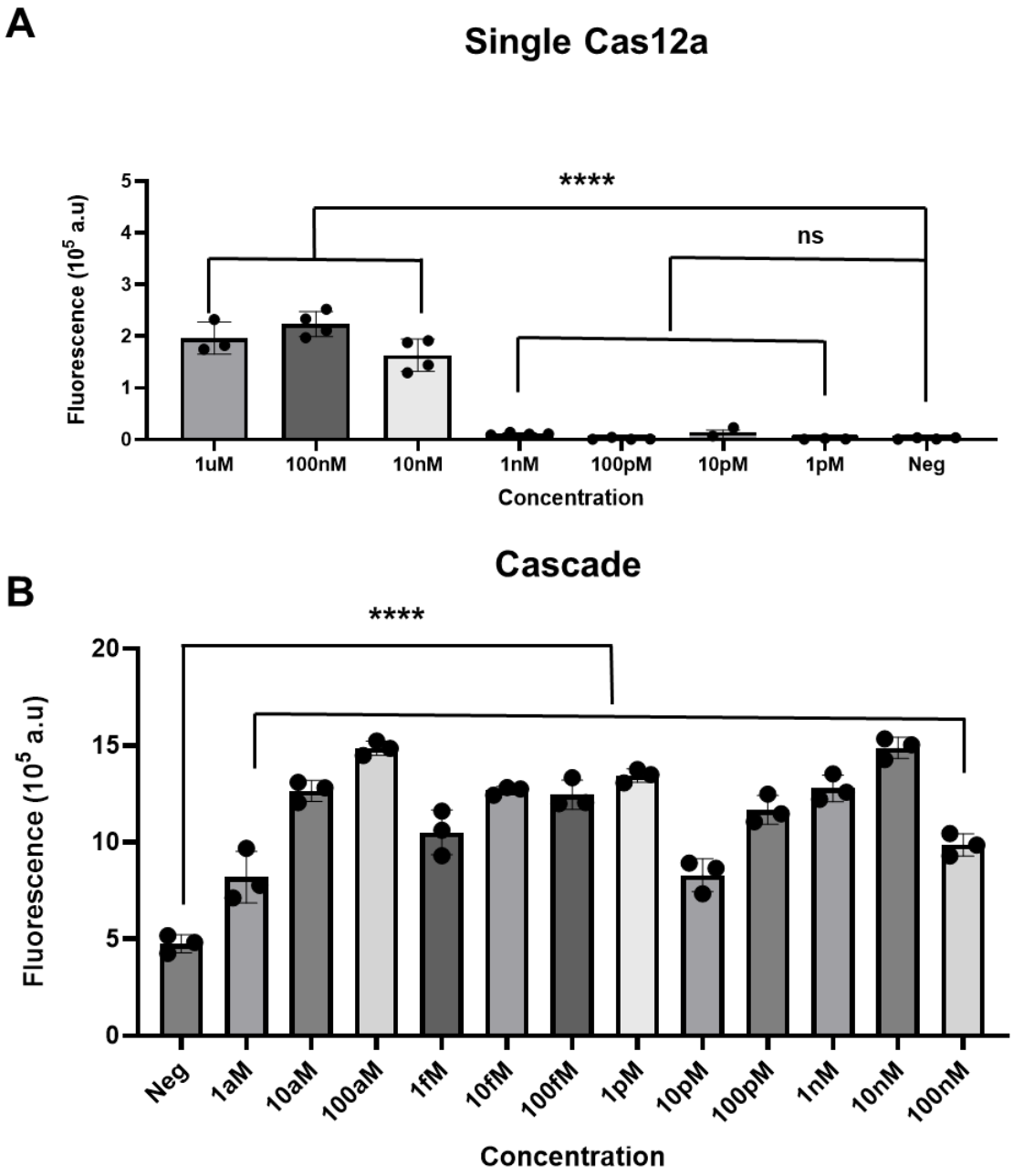


Figure S6. Ordinary one-way ANOVA test for the comparison of statistical difference of fluorescence signals at 360 mintues between negative and different concentrations of MRSA genomic DNA for (A) Single Cas12a reaction and (B) Cascade reaction. From the single Cas12a reaction, Dunnett's post-hoc test revealed that 1µM to 10nM differed significantly from the negative control. However, no significant differences were observed between concentration below 1nM and the control. From the Cascade reaction, Dunnett's post-hoc test revealed that all groups differed significantly from the negative control. Data are presented as mean ± SD (n=3 or 4), with a bar indicating the mean value. *p < 0.05, **p < 0.01, ***p < 0.001, ****p < 0.0001.

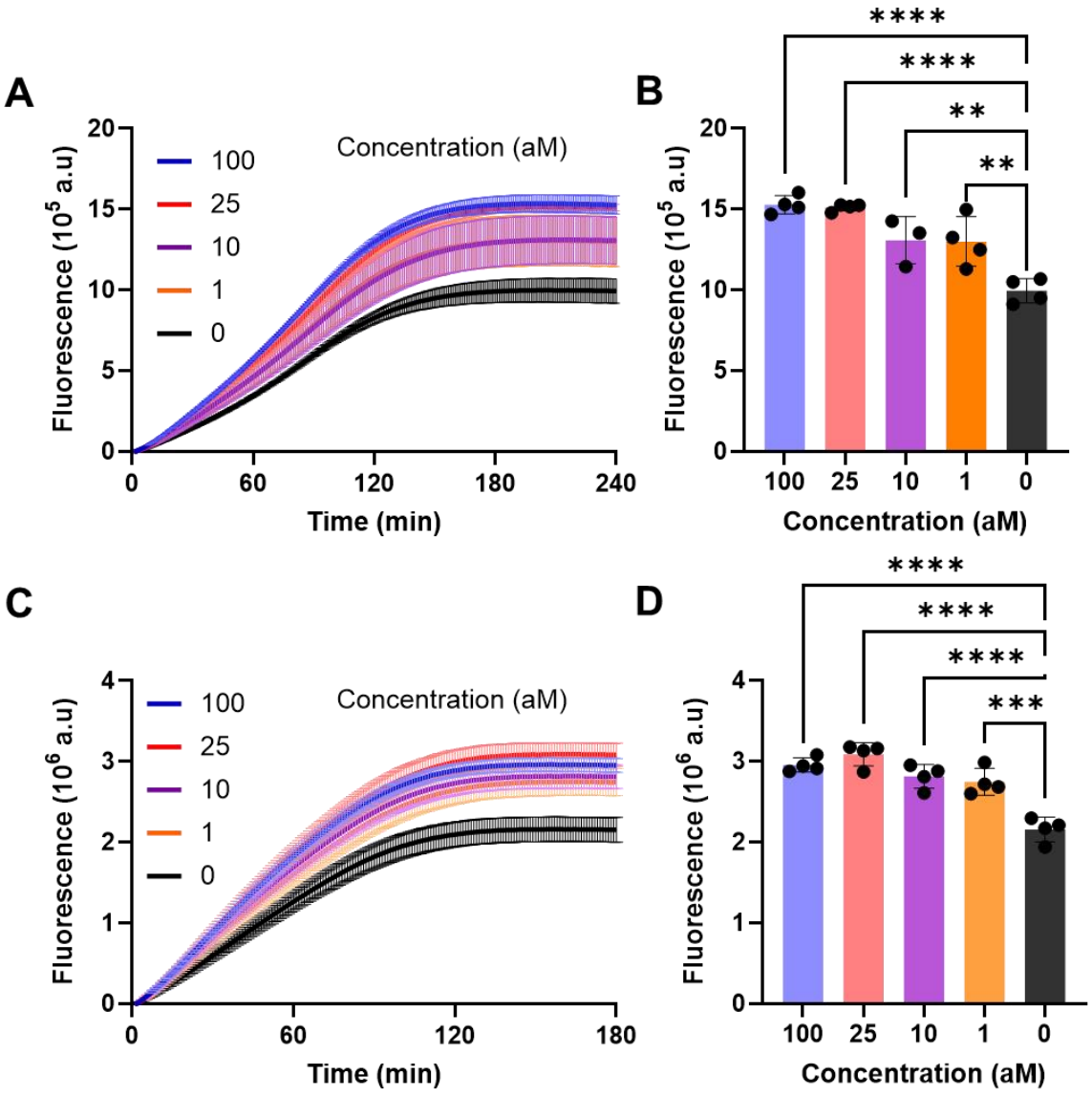


Figure S7. Fluorescence results from Cascade reaction experiments targeting a fragment of the MRSA mecA gene were observed over a period of 180-240 minutes. (A-B) An additional experiment was carried out to assess if signal quantification or a gradual increase (titration effect) occurs at atto-molar concentrations. (A) Displays raw fluorescence data, and (B) shows fluorescence levels at the 240-minute mark. (C-D) Additional experimental data are presented for 180 minutes. Data are presented as individual points with mean ± SD (n=3), with bars representing the mean value. An ordinary one-way ANOVA test was conducted to compare the statistical differences between the negative control and various concentrations of the MRSA mecA gene fragment. Dunnett's post-hoc test revealed that all groups significantly differed from the negative control. Data are shown as mean ± SD (n=3 or 4), with bars indicating the mean value. *$p < 0.05$, **$p < 0.01$, ***$p < 0.001$, ****$p < 0.0001$.

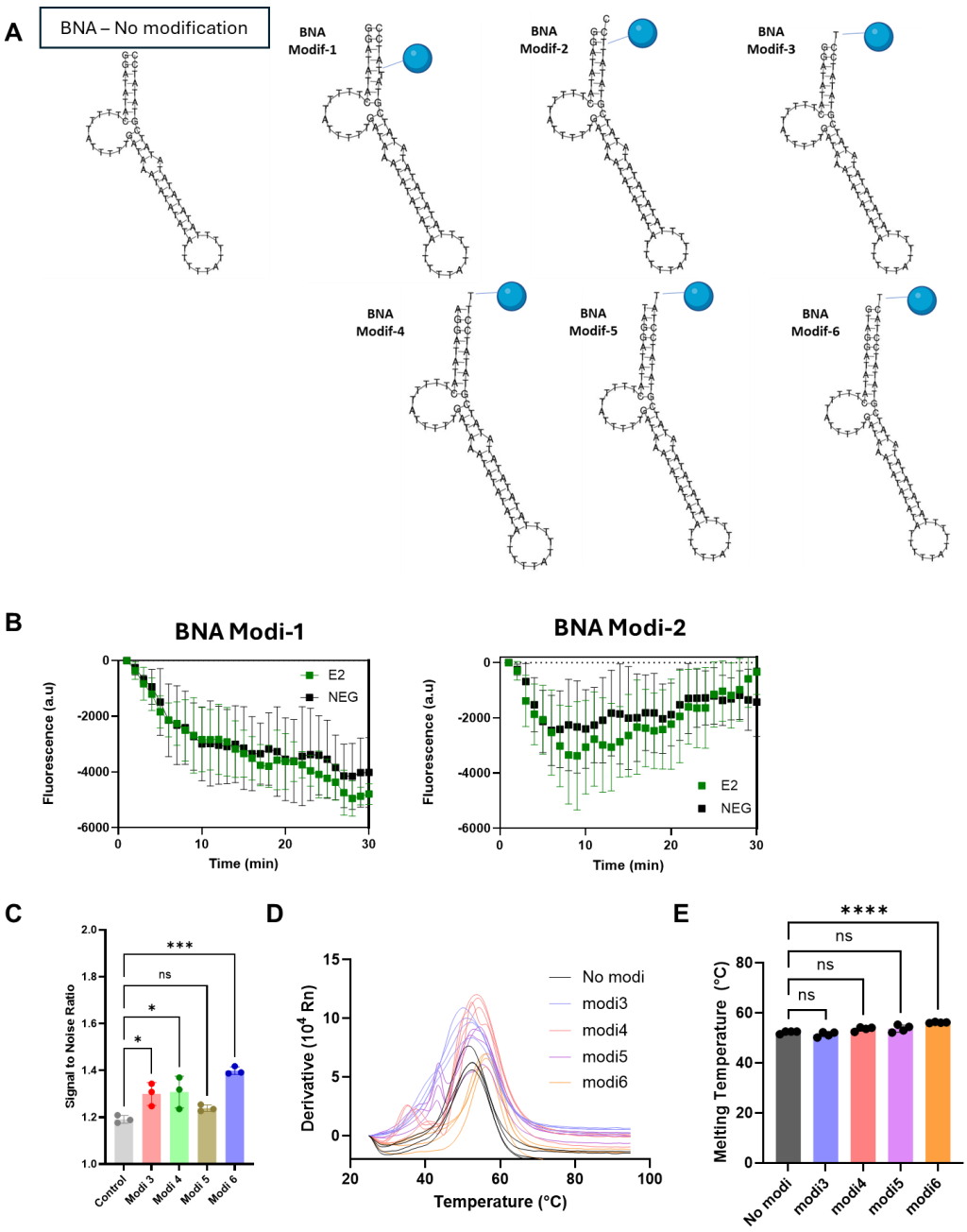


Figure S8. Biotin modification to BNA with different locations. (A) 6 different molecules with two of them (BNA Modi-1 and Modi-2) inserting biotin-T inside BNA molecules (B) Experimental results when using BNA Modi-1 and Modi-2 with noise signals without significant signal generation. (C) SNR of rest 4 molecules adding biotin-T at the end of the structure (BNA Modi-3 – Modi-6). Statistical analysis of 4 modification with original BNA molecules using the ordinary one-way ANOVA test. Modification group 3,4, and 6 differed significantly from the control. However, no significant differences were observed between modification 5 and the control. (D-E) Melting curve analysis was performed for BNA Modi-3 through Modi-6, in comparison to unmodified BNA. Among these, only the Modification 6 molecules showed a statistically significant difference. Data are presented as mean ± SD (n=3), with a bar indicating the mean value. *p < 0.05, **p < 0.01, ***p < 0.001, ****p < 0.0001.

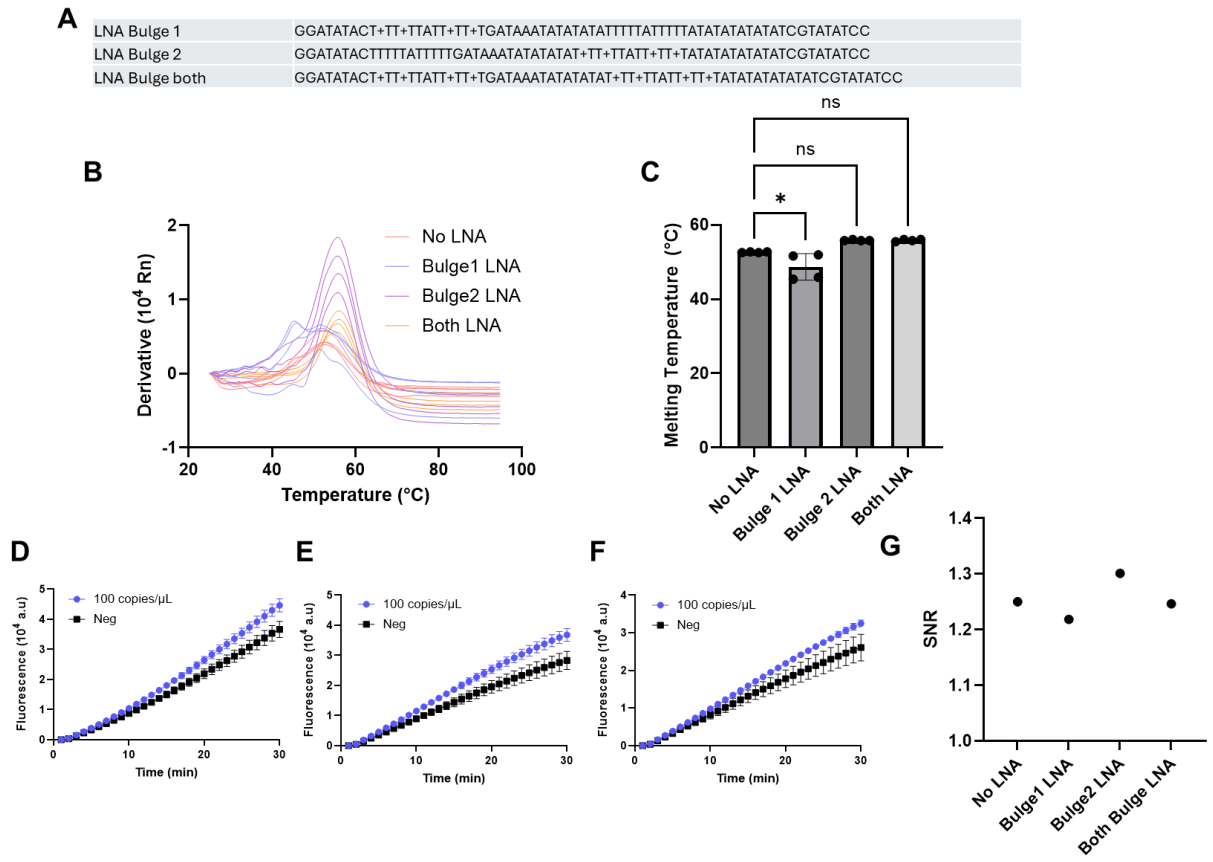


Figure S9. LNA modifications were introduced into the BNA within its bulge structure. (A) Nucleic acid sequences for different versions of LNA-modified BNA are shown, with '+' indicating LNA modifications. The LNA Bulge 1 molecule has LNA modifications at four distinct thymine residues, LNA Bulge 2 has the modifications at a different bulge location, and the LNA Bulge Both molecule contains a total of eight modifications across both sites. (B-C) Melting temperature analysis revealed no significant change in melting temperature due to LNA modifications. (D-F) Cascade reactions with 100 copies/µL and negative controls were conducted to determine if LNA modifications led to an improvement in signal-to-noise ratio (SNR). (G) The resulting SNR comparison between regular BNA (no LNA modification) and LNA-modified molecules was summarized. Statistical analysis of the melting curves, using 4 replicates and ordinary one-way ANOVA, showed no significant difference compared to the control (no LNA).For raw fluorescence measurements and SNR comparisons, 6 replicates were tested for each condition (100 copies/µL and negative control), with SNR comparison based on a single replicate. In general, SNR did not exceed 1.3.Data are presented as mean ± SD (n=3), with bars indicating the mean value. Statistical significance is indicated as *p < 0.05, **p < 0.01, ***p < 0.001, ****p < 0.0001.

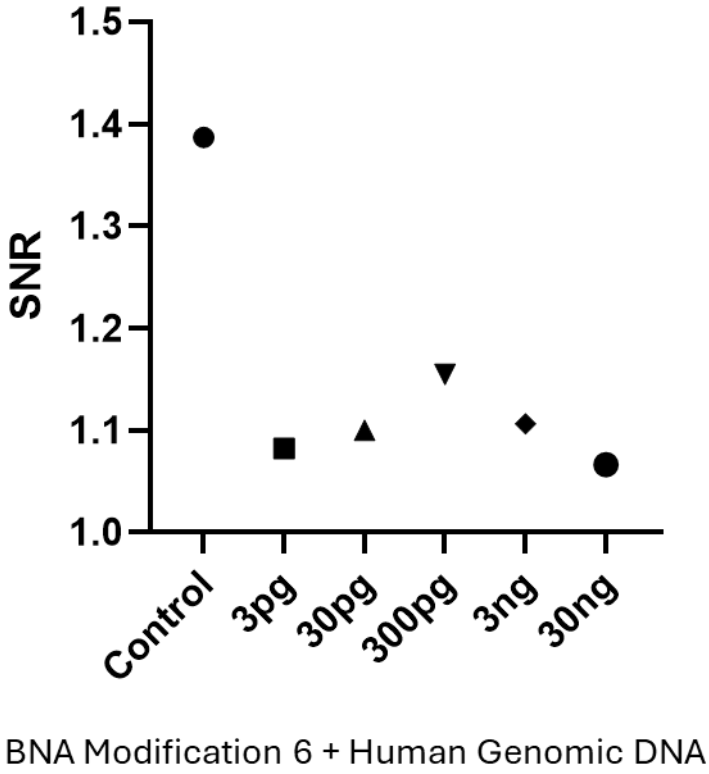


Figure S10. The combined effect of biotin modification and human genomic DNA on the SNR was assessed. While individually, both biotin modification of BNA and the inclusion of human genomic DNA in the sample increased the SNR, their simultaneous use unexpectedly led to a negative outcome. Specifically, a reduction in SNR was observed when testing BNA modification 6 with human genomic DNA concentrations ranging from 3pg to 30ng/µL. Only one replicate was tested for each condition.

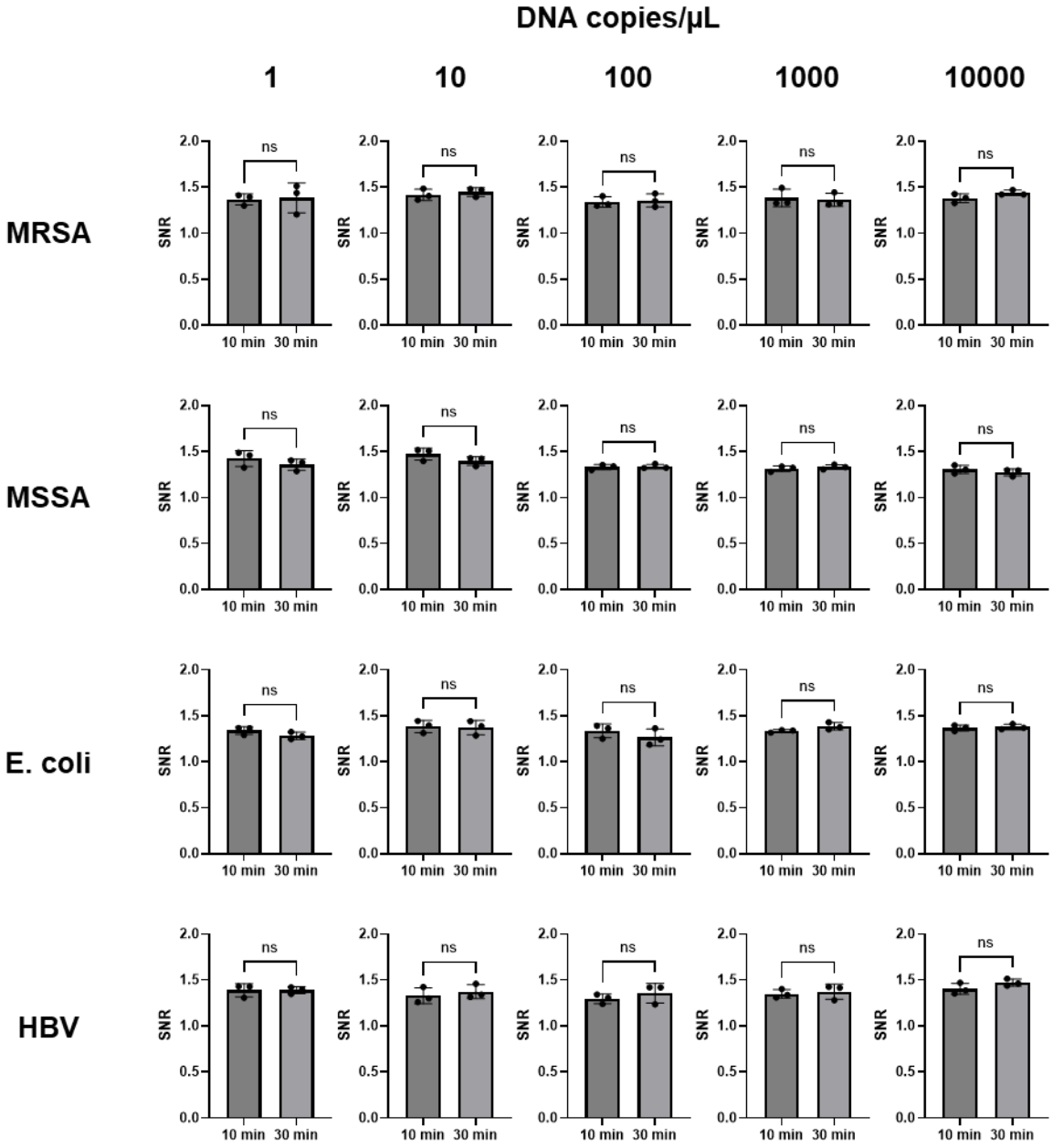


Figure S11. A statistical analysis of SNR was performed using an unpaired two-tailed t-test to compare the results between 10 and 30 minutes. The data are presented as mean ± SD (n=3), with bars representing the mean values. The notation 'ns' indicates no significant difference, meaning the p-value is >0.05.

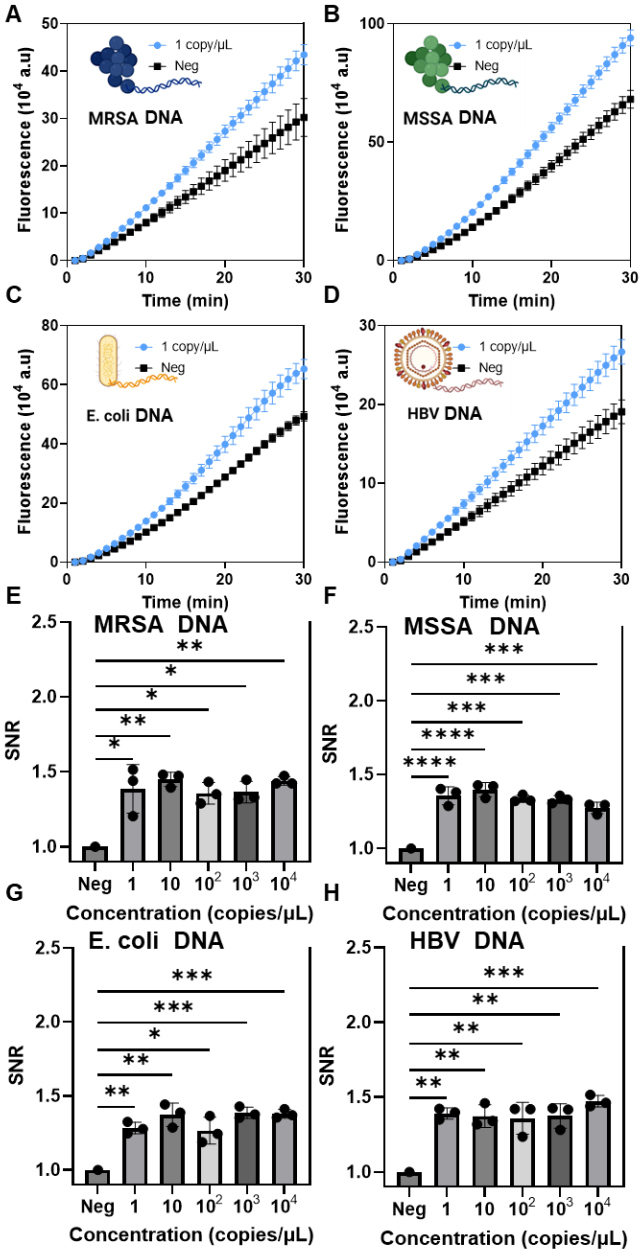


Figure S12. Development of cascade reaction for detecting various pathogenic DNA in water. (A-D) 1 copy/µL assay results for 30 minutes comparing positive to negative reactions using different gRNA-Target (gRNA T1): (A) MRSA, (B) MSSA, (C) E. coli, and (D) HBV. The points and error bars represent data collected from multiple wells. Corresponding SNR at 30 minutes for each pathogenic DNA in water with concentrations of 1 - 10^4 copies/µL: (E) MRSA, (F) MSSA, (G) E. coli, and (H) HBV. Each data point represents an individual experiment with multiple replicates. Data are presented as mean ± SD (n=3), with a bar indicating the mean value. Statistical analysis of all concentration was performed using the ordinary one-way ANOVA test and every concentration in every group differed significantly from the negative control. *p < 0.05, **p < 0.01, ***p < 0.001, ****p < 0.0001.

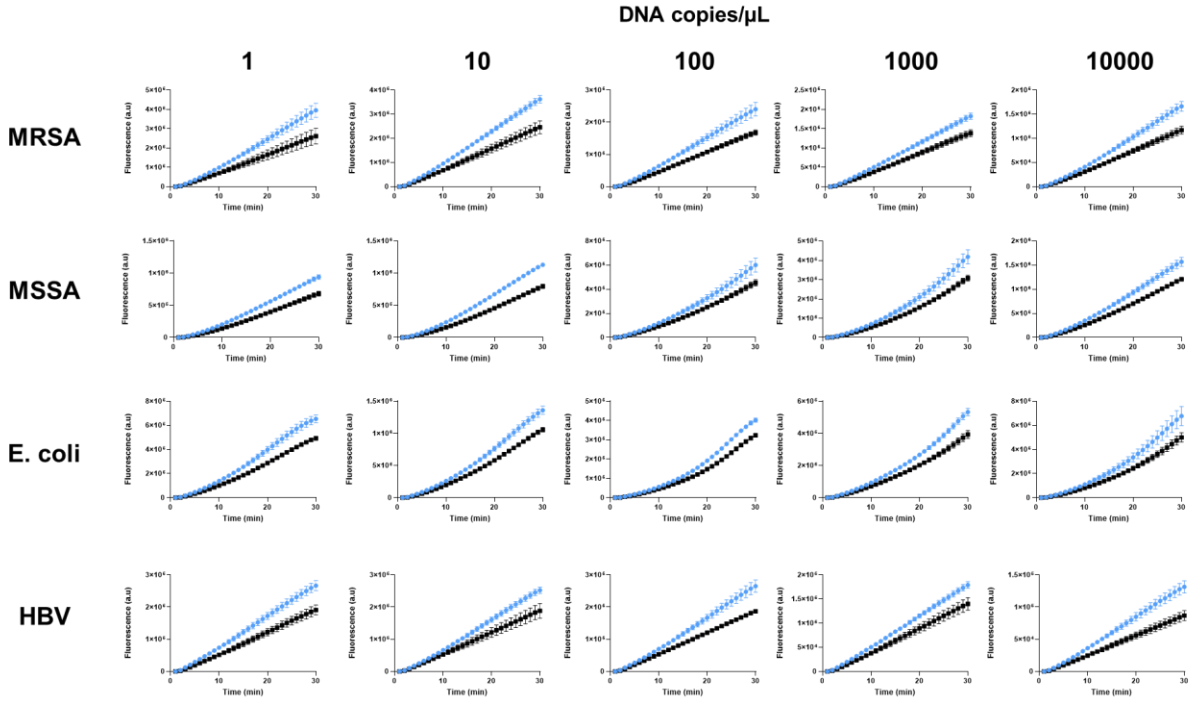


Figure S13. Development of cascade reaction for detecting various pathogenic DNA in water for MRSA, MSSA, E. coli, and HBV for 30 minutes for each pathogenic DNA in water with concentrations of 1 - 10^4 copies/µL. The points and error bars represent data collected from multiple wells. Data are presented as mean ± SD (n=3), with a bar indicating the SD value.

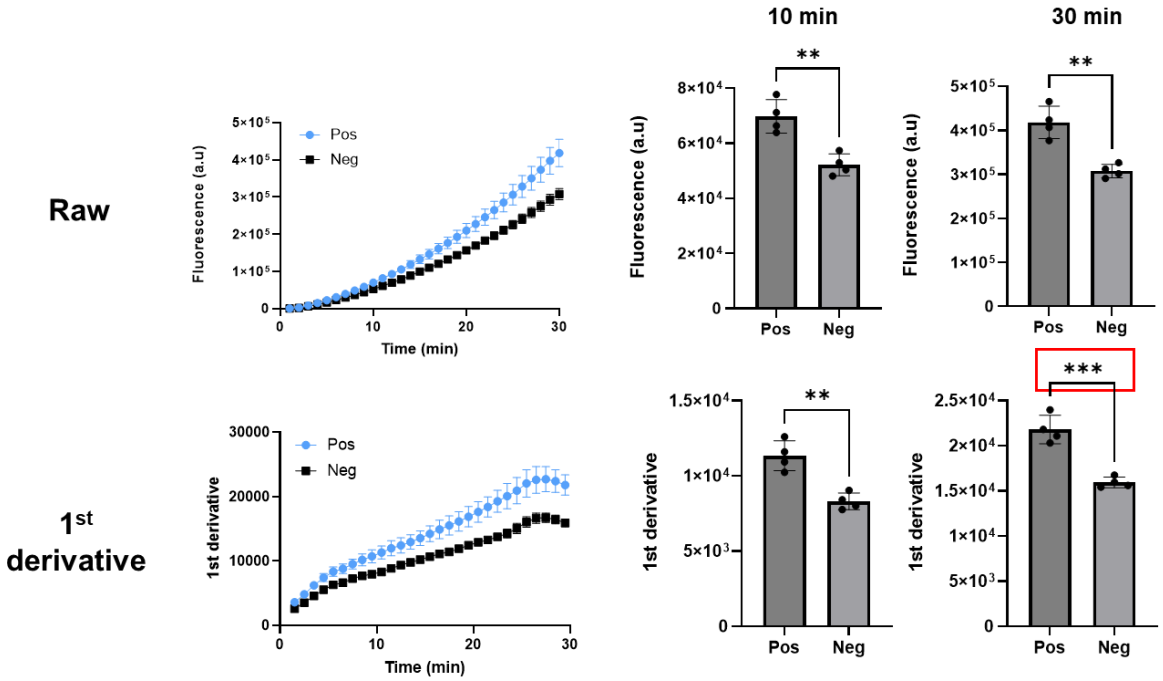


Figure S14. Applying the first derivative method to the raw data to potentially enhance discrimination capability. The points and error bars represent data collected from multiple wells. The red box emphasizes the enhanced discrimination effect. Data are presented as mean ± SD (n=3), with a bar indicating the mean value. Statistical analysis was conducted using a two-tailed unpaired t-test. The significance levels are indicated as follows: *p < 0.05, **p < 0.01, ***p < 0.001, ****p < 0.0001.

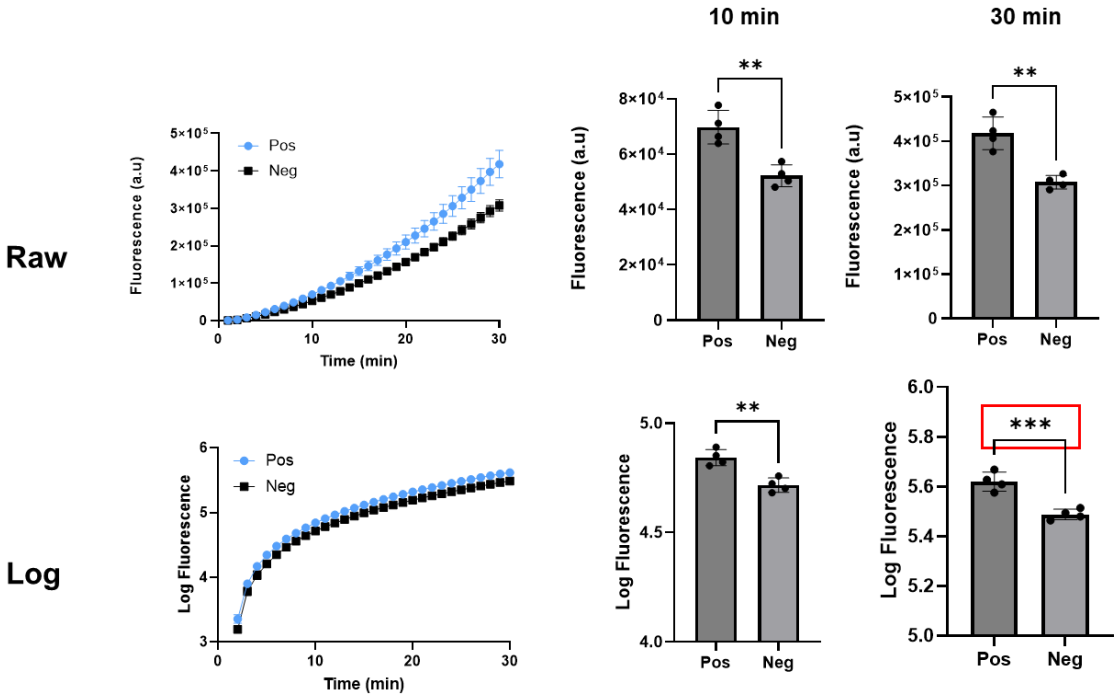


Figure S15. Utilizing the logarithm of the signal from the raw data to potentially improve discrimination capability. The red box emphasizes the enhanced discrimination effect. The points and error bars represent data collected from multiple wells. The red box emphasizes the enhanced discrimination effect. Data are presented as mean ± SD (n=3), with a bar indicating the mean value. Statistical analysis was conducted using a two-tailed unpaired t-test. The significance levels are indicated as follows: *p < 0.05, **p < 0.01, ***p < 0.001, ****p < 0.0001.

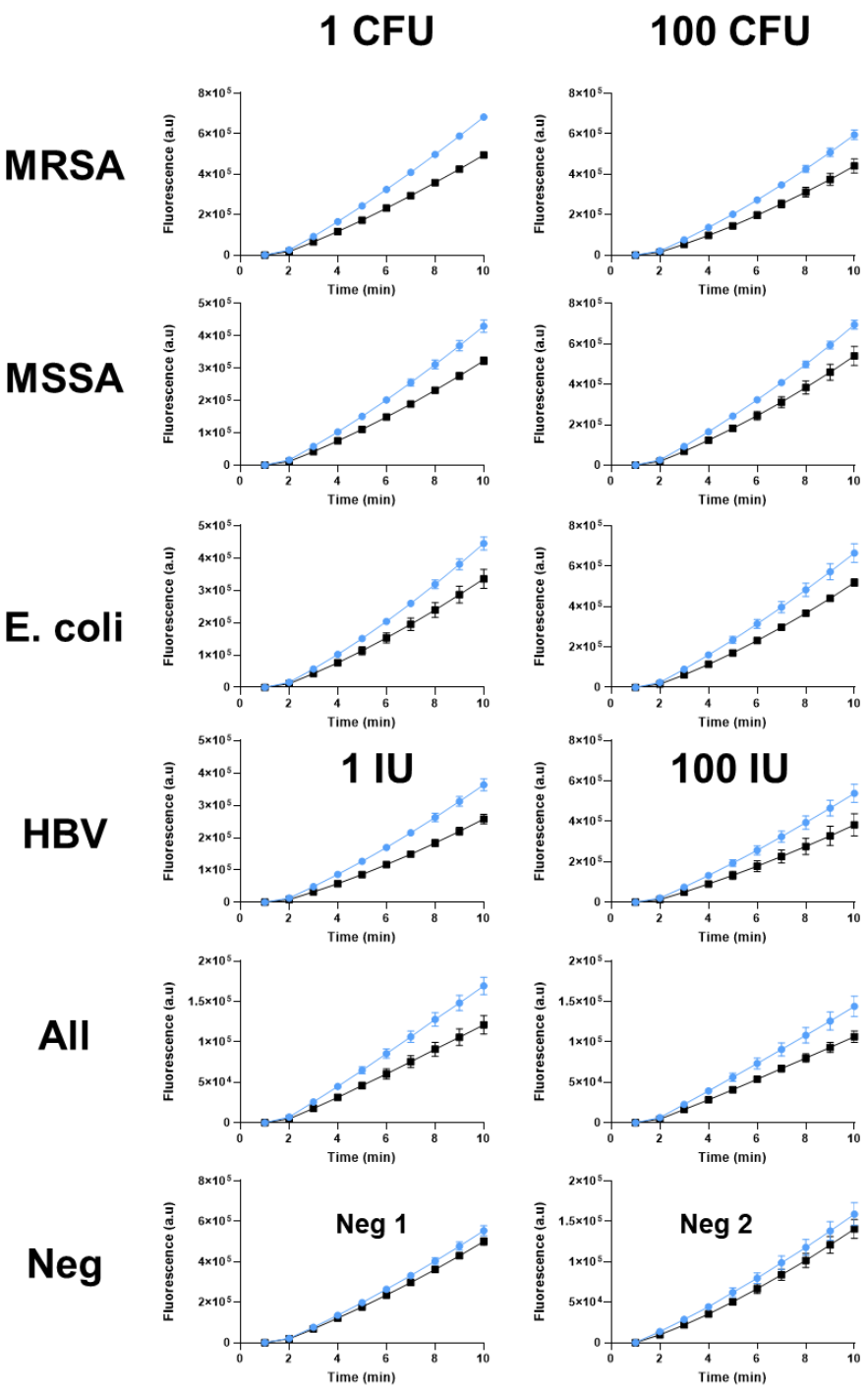


Figure S16. Development of cascade reaction for detecting pathogens in whole blood using extraction and purification. 1 and 100 CFU/µL assay results for 10 minutes comparing positive to negative reactions. (A) MRSA, (B) MSSA, (C) E. coli, and (D) HBV, and (E) negative control. 'All' in the panel refers to experiments conducted with samples containing all pathogens. The points and error bars represent data collected from multiple wells. Data are presented as mean ± SD (n=3), with a bar indicating the mean value.